GEOCAP Training Module

Understanding Electrical Properties of Rock

Geophysical method which measures resistivity structure of subsurface, is effectively proven for delineating geothermal system in exploration stage.

There are three types of conduction mechanism in the earth material, they are :

1. Electronic Conduction

   Electronic conduction is occurred in pure metals. The charge carriers are electrons that exist as a gas between ions and can move very easily through the metal. The resistivity is typically very low (~ 1.6 10 -8 Ωm).
2. Semiconductors

   Semiconduction is occurred in minerals such as sulphides. The charge carriers are electrons, ions or holes. The resistivity is usually higher (typically 10^{-3} to 10^{-5} Ωm). This type of conduction occurs in igneous rocks and usually shows a temperature dependence
3. Ionic Conduction in Liquids

   In liquids (aqueous fluids or molten materials) the ions can freely move. As the salinity of a brine increases, the resistivity decreases as more charge carriers become available.

The electrical resistivity, ρ, is defined through Ohm's law. The electrical field strength, E (V/m) is proportional to the current density, j (A/m^2):

$$E = \rho j$$

The proportional constant, ρ depends on the material and is called the electrical resistivity in Ωm. The reciprocal of resistivity is conductivity ($1/\rho=\sigma$). Resistivity can also be defined as the ratio of the potential difference, ΔV (V/m), to the current, I (A).

$$\rho \approx \frac{\Delta V}{I}$$

Factors that influence the electrical resistivity are porosity, temperature, salinity, and water-rock interaction. In porous rock with no clays and no matrix conductance, the resistivity of the rock will be controlled by the resistivity of the fluid (the saturating fluid). An empirical relationship between bulk resistivity (ρ), porosity (ϕ), water saturation (S_w) and fluid resistivity (ρ_w) has been widely used (Archie's law):

$$\rho = a\, \rho_w\, \Phi^{-n}\, S_w^{-m}$$

where a and n are constants (approximately 0.6 to 1.6 and 2 respectively) that are related to the character of the porosity. At saturations greater than 25%, m≅n.

In fact, there is no rock with clean matrix conductance and clay, so there is a modification of Archie's equation that includes a component for conduction by clay minerals within the matrix:

$$\rho = a\,\rho_w\,\Phi^{-n}\,S_w^{-m}\,(1 + KC\,\rho_w)^{-1}$$

where C is the proportion of clay minerals in the matrix and K is a constant according to the type of clay minerals present.

Waxman and Smits (1968) developed a quantitative relationship such that :

$$\rho = F/(B\,Q_v + \rho_w^{-1})$$

where F is formation factor, B is the equivalent conductance of counter ions (a function of solution conductivity), and Q_v is defined by :

$$Q_v = CEC(1 - \varphi) + \rho_m\Phi^{-1})$$

where ρ_m is matrix grain density and CEC is the cation exchange capacity of the clay in meq/gm. Typical CEC values for clays commonly found associated with geothermal systems are :

Table 1 : CEC Range in Clay Mineral (Ussher, 2000)

Clay Mineral	*CEC Range*	*CEC Average*
Kaolinite	3 - 15	10
Smectite (montmorillonites)	80 - 150	120
Illite	10 - 40	20
Chlorite	10 - 40	20

From the quantitative relationship by Waxman and Smits, it can be concluded that rocks containing smectite clays are likely to have resistivities 6 to 10 times lower than rocks with a similar proportion of illite (or chlorite) under the same temperature, porosity, and salinity conditions, and 12 times lower than rocks altered to kaolinite.

Commonly, clay contains electrolytes in its pores, so conduction is occured by ionic processes. Electrolyte resistivity is related to viscosity which decreases with temperature. Consequently ionic material has an inverse exponential dependence of resistivity with temperature of the form :

$$\rho = \rho_0\,e^{\frac{\varepsilon}{RT}}$$

where ε is an activation energy (commonly about 0.2 eV in water and for saturated rocks, varying with degree of alteration), R is Boltzman's constant (0.8617×10^{-4} eV/K), T is temperature (K).

Llera et al., (1990) tabulate decreases in laboratory measurements of resistivity in volcanic rocks by factors of 5 to 40 (commonly 6 to 10) for a temperature increase from 30 to 120°C.

The resistivity of saline fluids over the temperature range 20-350 °C has been well established experimentally (Ucok et al, 1980). Figure 1 shows the available data for a wide range of NaCl concentrations over the temperature range 20-400 °C and estimates a correlation contour among resistivity of brines, the measured salinity, and temperature range. The salinities of reservoir fluids from several well known geothermal fields are shown on this plot for reference.

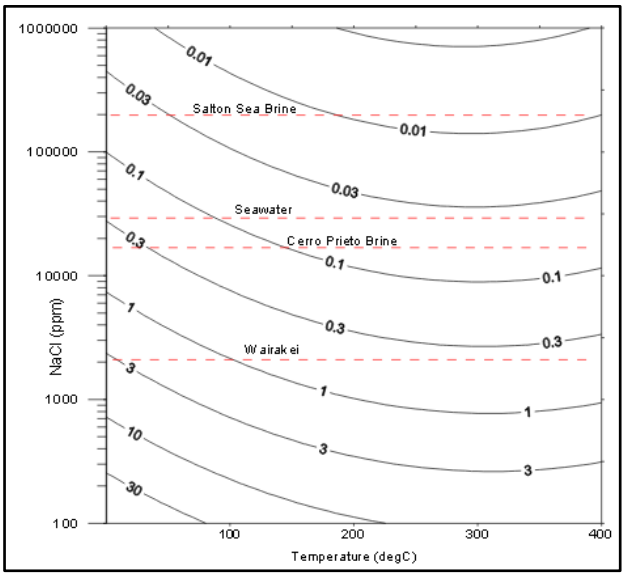

Figure 1: Variation of resistivity (in Ωm) of NaCl solutions from measurements of Ucok et al. (1980). (Ussher, 2000)

In geothermal system, low resistivity can be correlated with high salinity reservoir of geothermal system, however mainly correlated with clay hydrothermal alteration. The low resistivity zone at intermediate temperatures is often called cap rock and composes geothermal system. The high resistivity of the low-temperature zone tends to have poor water saturation, minimal hydrothermal alteration and little reduction of resistivity by temperature.

Correlation Between Geothermal System and Electrical Properties of Rock Formation

Geothermal systems consist of four main elements namely permeable reservoir rock, water to carry heat from the reservoir to the earth's surface, impermeable cap rock, and a heat source which depicted in Figure 2.

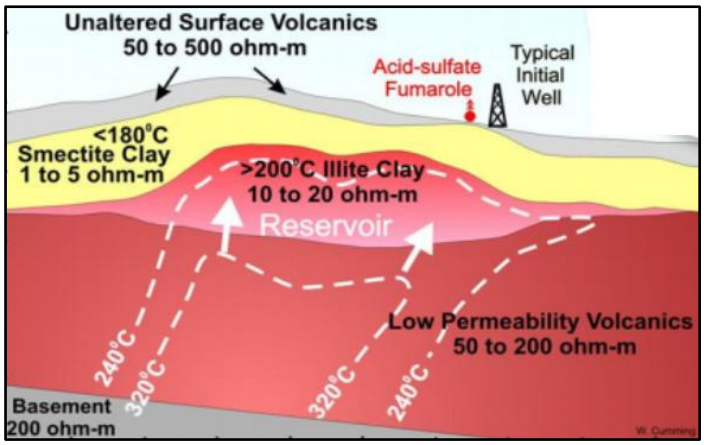

Figure 2: Geothermal system (Cumming, 2007)

In general, each element of geothermal systems has specific resistivity value. Impermeable cap rock is characterized by low resistivity (1 – 5 ohm-m, generally ≤ 10 Ωm). Resistivity value in impermeable cap rock is influenced by hydrothermal process which cause formation of clay alteration as cap rock. One of the most influential factors of resistivity value in clay is caused by containing cation exchange capacity of clay (CEC). Figure 2 shows that smectite clay has lower resistivity value than illite clay, and it is proven by containing of CEC in smectite clay is higher than illite. Reservoir rock has higher resistivity value than impermeable cap rock with resistivity about of 20-60 Ωm. Majority of heat source is volcanic rock with resistivity more than 100 Ωm.

The Fundamental of Magnetotelluric Technique

Magnetotelluric (MT) technique is a passive geophysical technique that utilizes electromagnetic waves in order to determine the electrical resistivity structure of the Earth's subsurface with penetration ranges from several meters to hundreds of kilometers through the measurement of electric field (E) and magnetic field (B) which are varied in time.

MT has been popular for geothermal exploration, mineral exploration, hydrocarbon exploration and regional geophysical mapping. It is used in oil exploration for low-cost reconnaissance of sedimentary basins and for exploration in areas where seismic surveys are difficult because of severe topography or the presence high-impedance volcanic rocks near the surface.

Magnetotelluric technique uses the concept of electromagnetic waves which propagates in conductive medium by utilizing the Maxwell's equations, including :

$$\nabla \times \overline{E} = -\frac{\partial \overline{B}}{\partial t}$$

$$\nabla \times \overline{B} = \mu\sigma\overline{E} + \mu\varepsilon\frac{\partial \overline{E}}{\partial t}$$

where the first equation is well-known called Faraday'equation and the second equation is Ampere's equation.

Faraday's equation shows how a time varying magnetic field can create an electric field orthogonal to it. Ampere's equation shows how an electric field can create a magnetic field orthogonal to it. Electric current can be generated by the movement of magnetic poles in conductor or the movement of conductor in magnetic poles which will produce changes in magnetic flux. According to Faraday's equation, changing of magnetic flux can generate electric current. So that, only time varying magnetic field that used in MT technique.

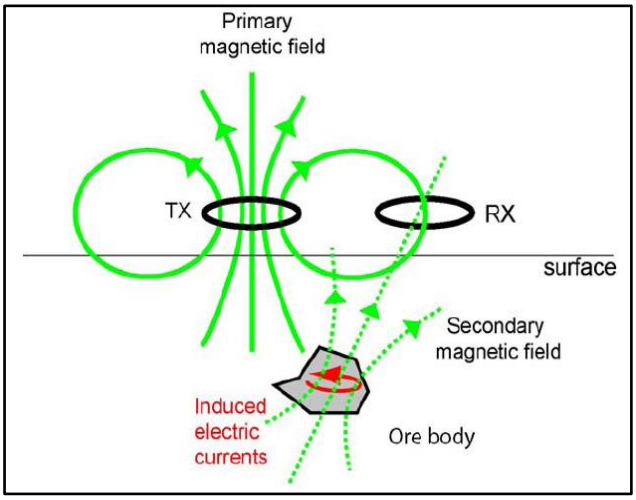

Figure 3: Basic concept of MT

Figure 3 shows that time varying electromagnetic field will induce rock in the Earth's subsurface and produce telluric current. Furthermore, telluric current generates secondary electric field and magnetic field which will be received by electrical and magnetic sensor.

Electromagnetic signals propagate by diffusion when it enter the Earth. The time varying magnetic field induces electric current. As the electric current flows, energy is converted to heat and cannot be converted back. This causes the ampitude of electromagnetic signals are decreased. Skin depth is characteristic of depth where electromagnetic waves amplitude are reduced to 1/e amplitude on the Earth's surface. Skin depth can be approximated as :

$$\delta = 503 \sqrt{\frac{\rho}{f}}$$

Case Study-Mt. Pancar

Mt. Pancar geothermal prospect is located in the Bogor District, West Java Province, Indonesia about 40 km to the south of Jakarta (Figure 8). The geological conditions of the area consist of Tertiary volcanic formation of the Mt. Pancar and Quaternary volcanic formation of Mt. Panisan covering Tertiary sedimentary formation as basement (Figure 9). The geological structure is dominated by northwest – southeast structure orientation (Figure 9). The surface manifestations found in this geothermal area are hot springs, warm grounds and altered rocks controlled by a fault structure. The hot springs are found in Kawah Merah (T = 70^{o}C) and Kawah Putih (T = 51^{o}C) with neutral pH and minor silica sinter. There is no indication of thermal activity on the summit of Mt. Pancar. The subsurface temperature, as indicated by Na/K geothermometry, is in the range of 180-190^{o}C. Based on the preliminary information, it can be concluded that the Mt Pancar geothermal area can be classified as a low to moderate geothermal resource.

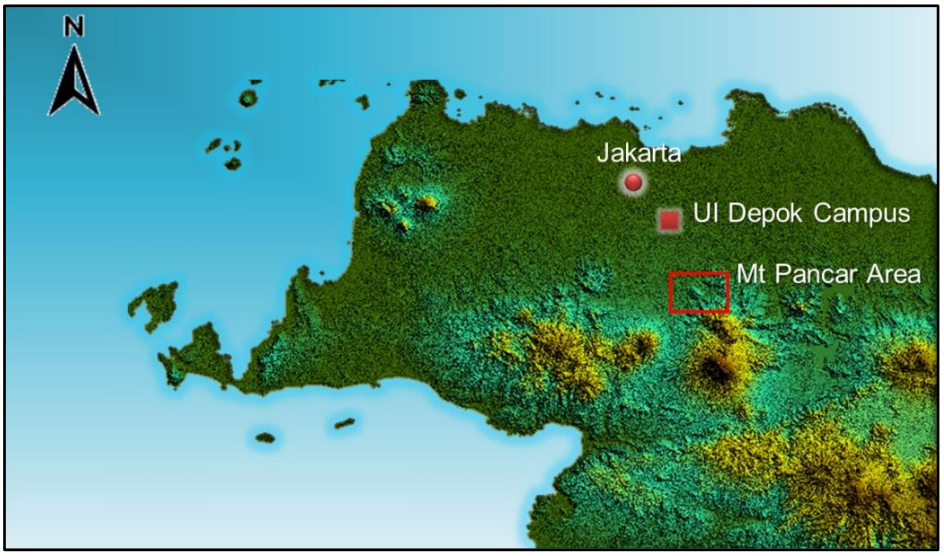

Figure 8: Location Map of Mt. Pancar Geothermal Prospect Area (Daud et al., 2015).

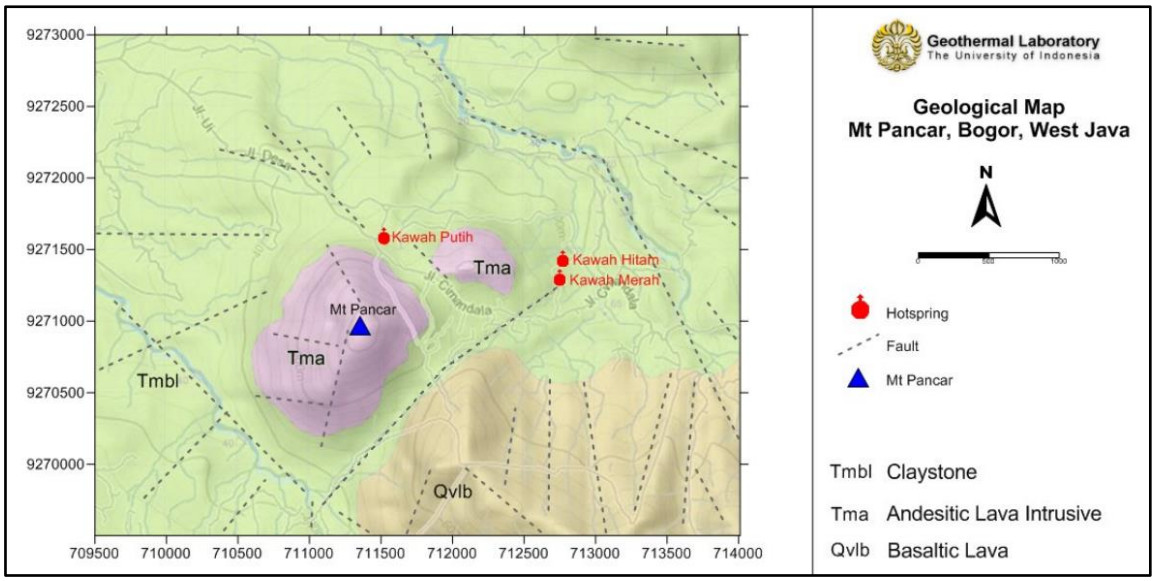

Figure 9: Geological Map of Mt. Pancar Geothermal Prospect Area (Daud et al., 2015).

The geophysical survey is utilized to develop an initial conceptual model of the Mt. Pancar geothermal system. Ten sounding of AMT data were accomplished along two profiles both crossing Mt. Pancar summit and the other ends crossing Kawah Merah (Line AB) and Kawah Putih (Line CD) hot springs area, respectively (Figure 10). The AMT survey was conducted using Phoenix equipment system. The duration of measurement was about 2 hours per station. The frequency range is from 0.1 Hz to 10 kHz. Data processing was carried out using SSMT2000 software. The AMT data quality was good to excellent. 2-D and 3-D inversions of the AMT data were then carried out along the profile lines using WinGLink software and MT3DInv-X, respectively. Results of 3-D inversion of AMT data was integrated to develop a conceptual model of Mt. Pancar geothermal prospect area.

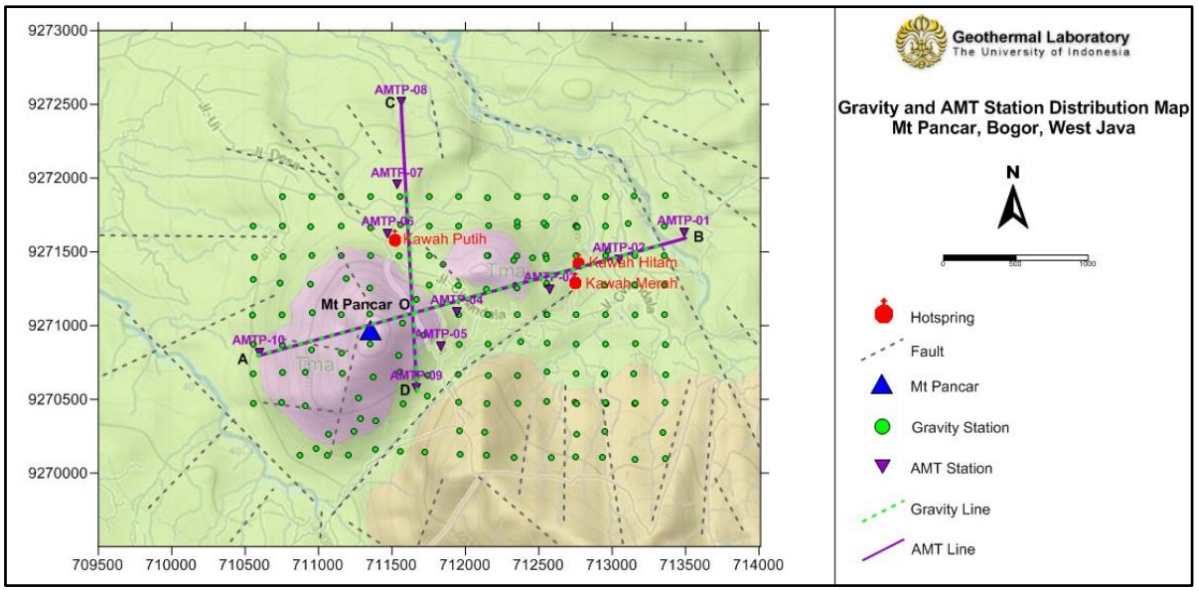

Figure 10: Distribution of Gravity and AMT Measurement Stations in Mt Pancar Geothermal Prospect Area (Daud et al., 2015).

The AMT data was inverted using 3-D inversion algorithm to get the subsurface true resistivity distribution. As shown in the two profiles, the subsurface resistivity distribution in the Mt. Pancar area is dominated by low resistivity layer (< 15 ohm-m) distributed from near surface down to about 2000 meter depth. The low resistivity layer is interpreted as the clay cap of the Mt. Pancar geothermal system distributed between Mt. Pancar and Kawah Merah (Line AB; Figure 11) and between Mt. Pancar and Kawah Putih (Line CD; Figure 12). The up-dome shape of the base of the conductive layer indicates an upflow zone. The slightly resistive layer (20 – 100 ohm-m) was also found underlying the clay cap which is interpreted as a reservoir zone. The more resistive basement (> 100 ohm-m) was encountered forming graben-like structure as indicated by the gravity data. The graben-like structure possibly controls the hydrothermal system in Mt. Pancar area as indicated by the occurrence of hot springs.

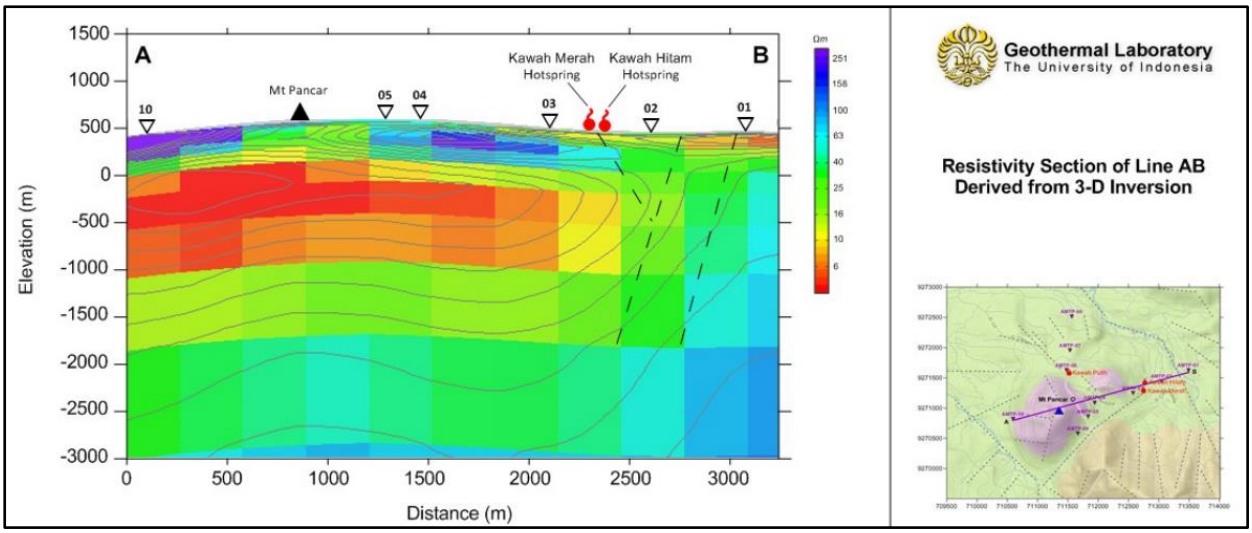

Figure 11: Resistivity Section Derived from 3-D Inversion of AMT Data (Line AB) (Daud et al., 2015).

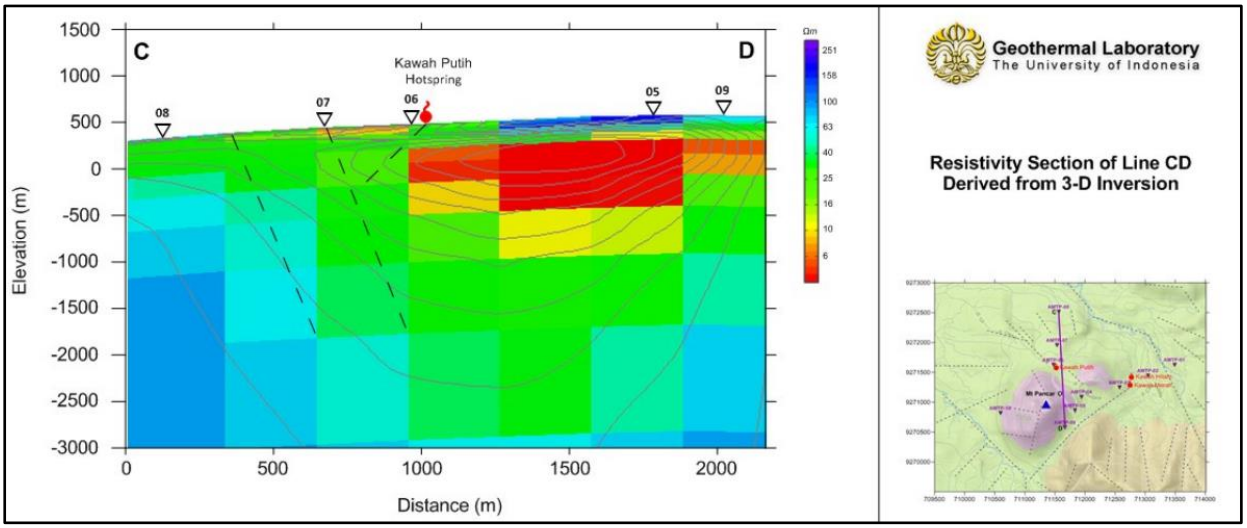

Figure 12: Resistivity Section Derived from 3-D Inversion of AMT Data (Line CD) (Daud et al., 2015).

Interpretation was then accomplished by incorporating AMT supported by geological and geochemical data to develop the conceptual model of the Mt. Pancar Geothermal Area. Figure 13 shows the conceptual model of Mt. Pancar geothermal area. The possible up-flow zone is inferred in the vicinity of Mt. Pancar summit as indicated by the up-dome shape of the conductive layer. While the outflow zone is indicated towards the north where the Kawah Putih hot spring occurs, as well as towards the east, where the two hot springs, Kawah Merah and Kawah Hitam, are found. There is still a crucial question concerning the inference of the up-flow zone, since no surface manifestation is found in the vicinity of Mt. Pancar summit. Temperature gradient drilling should therefore be recommended in this location to confirm the subsurface temperature.

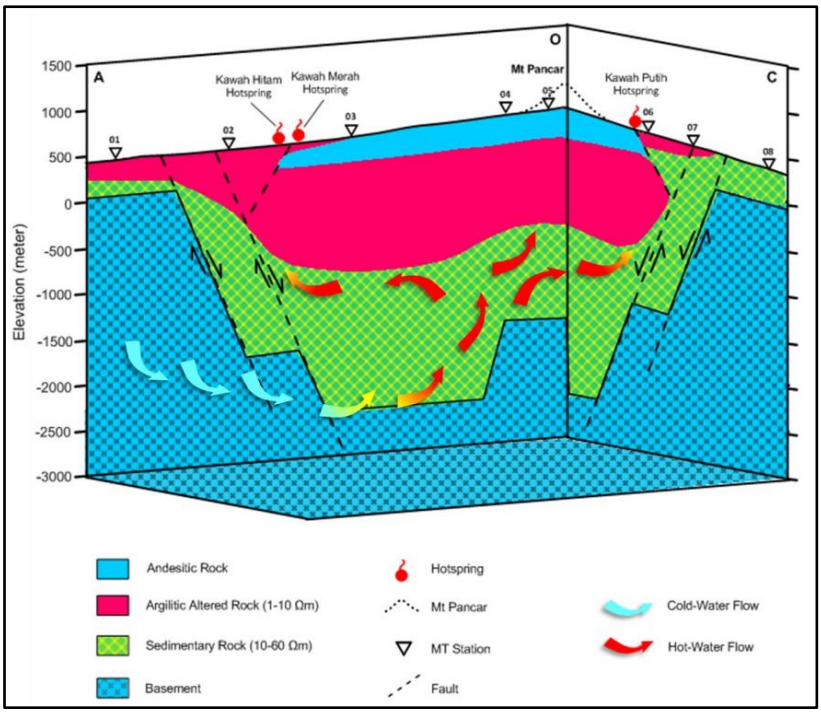

Figure 13: Conceptual Model of Mt Pancar Geothermal Prospect Area (Daud et al., 2015).

Case Study- 3-Dimensional Inversion of MT Data over the Arjuno-Welirang Volcanic Geothermal System, East Java (Indonesia)

The Arjuno-Welirang geothermal area is located about 60 km southwest of Surabaya, the capital city of East Java (Figure 14). The presence of a geothermal system in this area is related to the volcanic activity in the south of East Java. Geologically, the prospect area is dominated by Quaternary volcanic rocks, both lava and pyroclastic. Geological structures such as faults, the caldera rim structure, and other circular features are indicated by remote sensing data. The circular feature is correlated with the collapse zone that was formed as a result of Pre Arjuno-Welirang volcanic eruption (Figure 15).

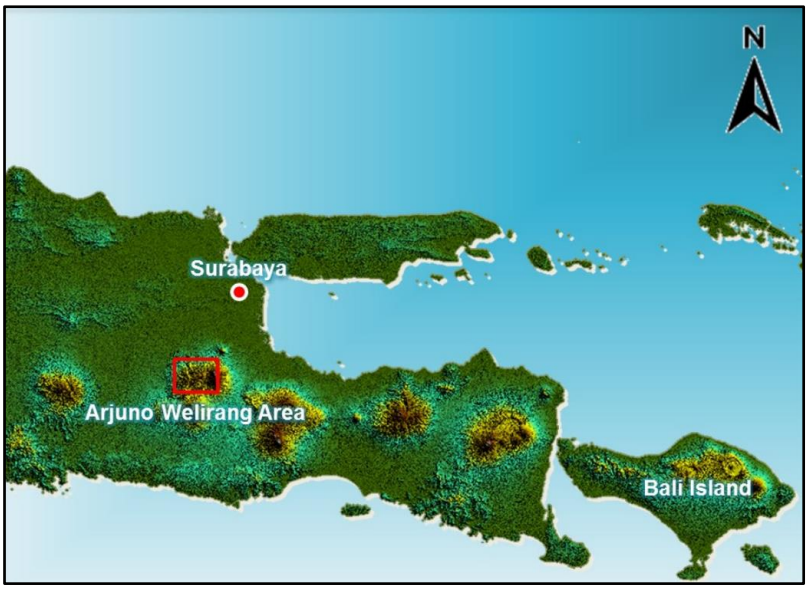

Figure 14: Location of Arjuno-Welirang Geothermal Area, East Java, Indonesia (Daud et al., 2015).

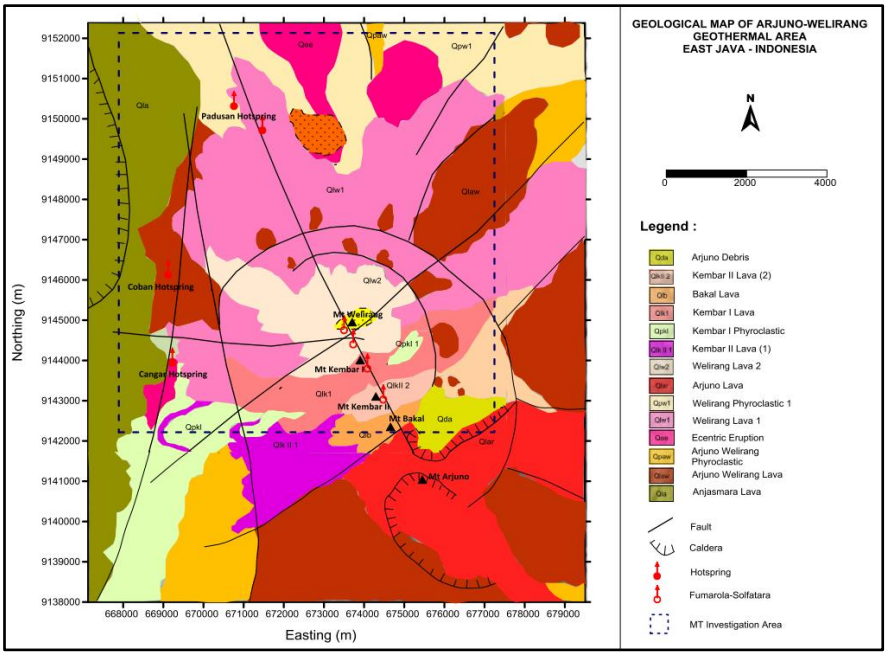

Figure 15: Geological Map of Arjuno-Welirang Geothermal Area, East Java, Indonesia (Daud et al., 2015).

Impressive surface thermal manifestations are found in this area included solfataric-fumaroles with a temperature of 137°C found in the summit of Mt. Welirang. In addition, bicarbonate hotsprings with temperature values ranging from 39 to 55°C were found in the western and northwestern vicinities of Mt. Welirang. In the Na-K-Mg diagram (Figure 16), all of the hotsprings were determined as immature water, indicating the mixing of thermal water and shallow ground water. The outcrop of advanced argilic alteration was found in the summit of Mt. Welirang,

whereas the outcrop of weak argilic alteration was found in the vicinites of Mt. Pundak. The occurrence of solfataric-fumaroles with magmatic gases indicated the existence of a volcanic geothermal system in the subsurface. Cangar and Coban hotsprings were controlled by Cangar faults, whereas the Padusan hotsprings and solfatara-fumaroles were controlled by the Padusan faults. The temperature of the reservoir, assessed using gas geothermometers, was about 260°C. Therefore, the Arjuno-Welirang geothermal system could be categorized as a high temperature geothermal system.

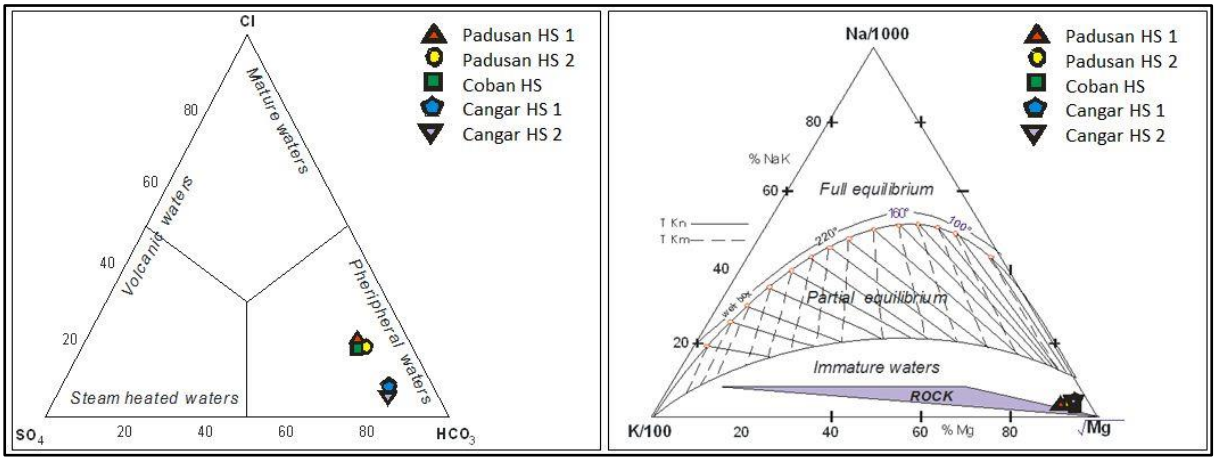

Figure 16: Ternary Diagram of Chemical Compositions of Hot Springs in the Arjuno-Welirang Geothermal Area (Daud et al., 2015).

The 3-D inversion method was applied for the 34 MT soundings with a frequency range of 100 to 0.01 Hz. The overall quality of the MT data used varied from good to very good. The 3-D MT inversion was carried out using the MT3DInv-X software program (Daud et al., 2012). It is a user-friendly software program that utilizes the Occam's inversion data space algorithm developed by Siripunvaraporn (2011). With this software program, the 3-D inversion process was performed more effectively. The result of the 3-D inversion in this software program was integrated with the GeoSlicer-X software program (Daud and Saputra, 2010). The output of the MT3DInv-X was exported into the (x, y, z) value data format, which was used as data input in the GeoSlicer-X software to visualize the data in three dimensions.

The subsurface resistivity structure revealed by the 3-D inversion process indicated the presence of geothermal system in this area. The conductive layer, one of the characteristics of a geothermal system, is found in the resistivity model. This can be seen in the cross-section Line AB (Figure 17) and cross-section Line CD (Figure 18). This conductive layer has a resistivity between 1 to 15 ohm-m with various thickness values that range from 1 to 2 km. The slightly higher resistivity layer below the conductive layer has a resistivity of 20 to 60 ohm-m. The lower part of the resistivity

structure shows the highest resistivity value that is greater than 80 ohm-m. The geometry of the resistivity structure shows an updome structure for the base of conductive layer (BOC) centered below Mt Welirang. The resistivity contrast in the cross section indicates the geological structures, such as faults, in this area.

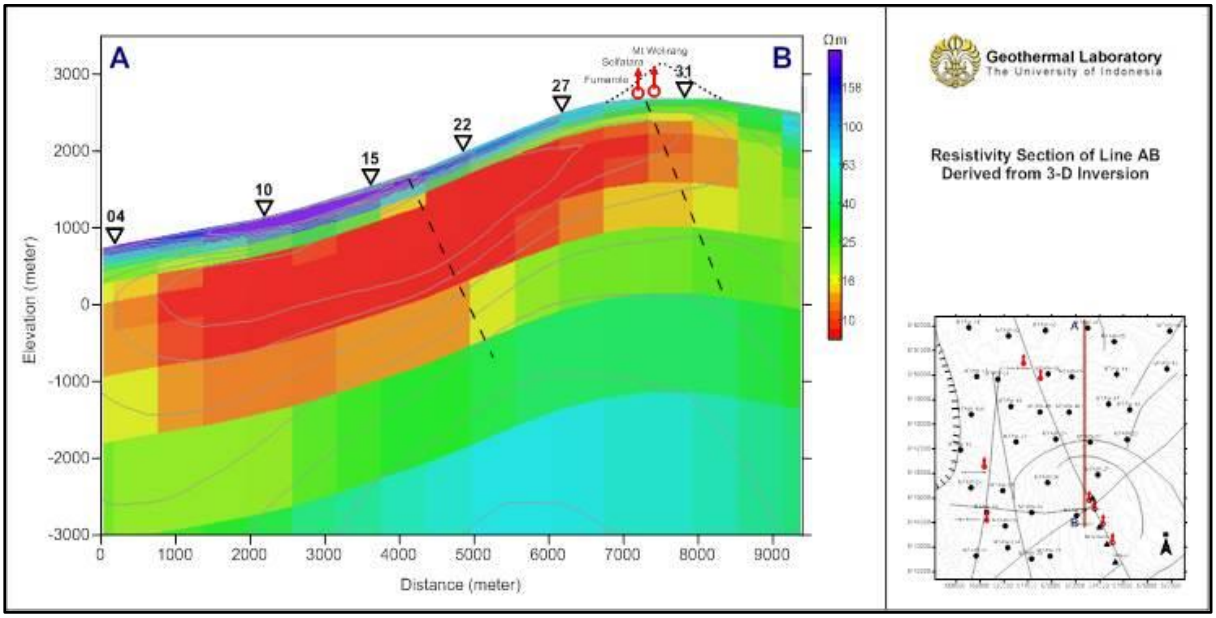

Figure 17: Resistivity Structure Derived from 3-D Inversion along Line AB of the Arjuno-Welirang Geothermal Area (Daud et al., 2015).

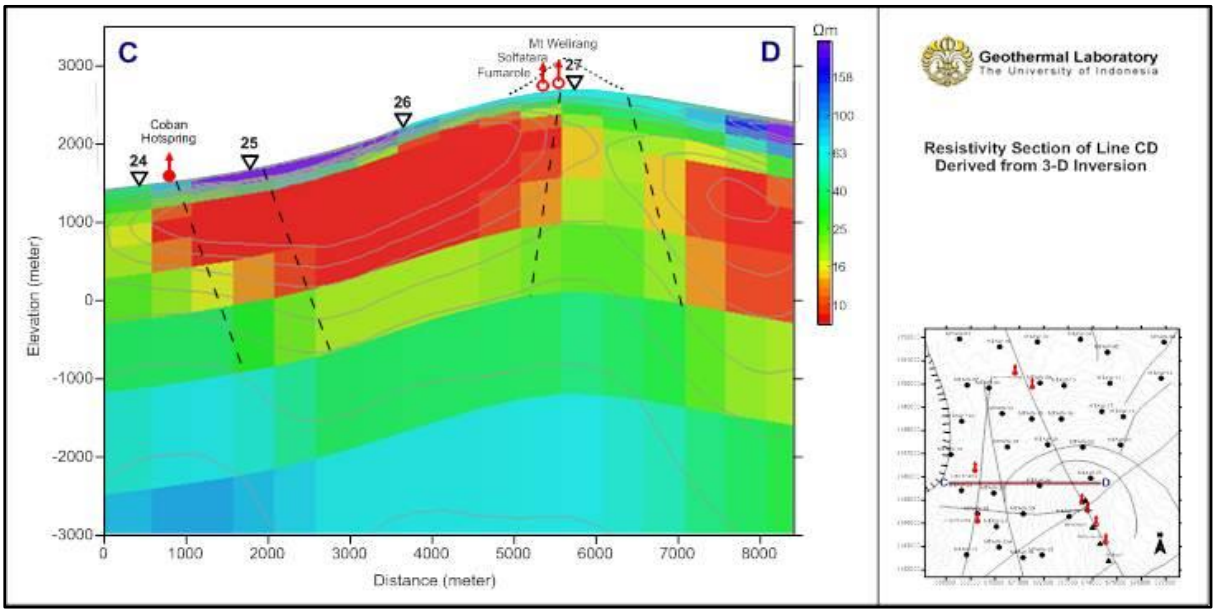

Figure 18: Resistivity Structure Derived from 3-D Inversion along Line CD of the Arjuno-Welirang Geothermal Area (Daud et al., 2015).

Integrated interpretation was done to develop a conceptual model of Arjuno-Welirang geothermal system. The 3-D MT inversion result was then incorporated with the geological and geochemical data. Magnetotelluric investigation is necessary for identifying the existence of upflow and outflow zones, as well as the indicated geological structures. The upflow zone is clearly indicated by the updome resistivity structure of the Line AB and Line CD below Mt. Welirang (Figure 17 and Figure 18). The presence of solfataric-fumaroles in the summit of Mt. Welirang supports the interpretation of the upflow zone location. In addition, the occurrence of solfataric-fumaroles with magmatic gases indicates that the upflow zone originates from a volcanic geothermal system in the subsurface. The outflow structure is also indicated clearly by the elongation of the conductive layer in the resistivity sections of the Line AB and Line CD (Figure 17 and Figure 18), following the decrease in surface topography. Chemical compositions analysis results from the Cangar hotsprings, Coban hotsprings, and Padusan hotsprings supports the indicated outflow zones. Electrical discontinuities in the resistivity sections of Line AB and Line CD can be interpreted as faults represented by dashed lines (see Figure 17 and Figure 18). These fault structures might control the upflow and outflow zones in the Arjuno-Welirang hydrothermal system. Figure 19 summarizes the 3-D resistivity model and its interpretation for the Arjuno-Welirang geothermal system using the Geoslicer-X software (Daud et al, 2010).

On the basis of the integrated interpretation of the 3-D inversion of the MT data incorporated with geological and geochemical data, a conceptual model of Arjuno-Welirang geothermal system was then developed, as shown in Figure 20 and Figure 21. Figure 20 illustrates the conceptual model represented by the base of conductor (BOC) elevation contour and possible hydrogeology. In addition, Figure 20 shows the conceptual model represented by the subsurface distribution of altered rocks, reservoir rocks, fault structures, and possible hot rocks. The main upflow zone is situated below the Arjuno-Welirang volcanic complex, as indicated by the highest elevation of BOC (Figure 20) and updome shape of the conductive layer, as well as horst structure of the resistive basement interpreted as hot rock (Figure 21). The occurrence of solfataric-fumaroles with magmatic gases in the summit of Mt Welirang supports this model and indicates that the upflow zone originates from a volcanic geothermal system in the subsurface. The main reservoir below MT Welirang is located at a depth of about 1,500 meters. Furthermore, the subsurface temperature at this depth, estimated from gas geothermometry, is about 260^{o}C. The conceptual model also suggests that the outflow zones are situated in three locations: Padusan, Cangar and Coban area as indicated by the occurrence of hot springs in the areas. The existence of the outflow zones are controlled by the northwest-southeast and west-east fault structures (Figure 20 and Figure 21).

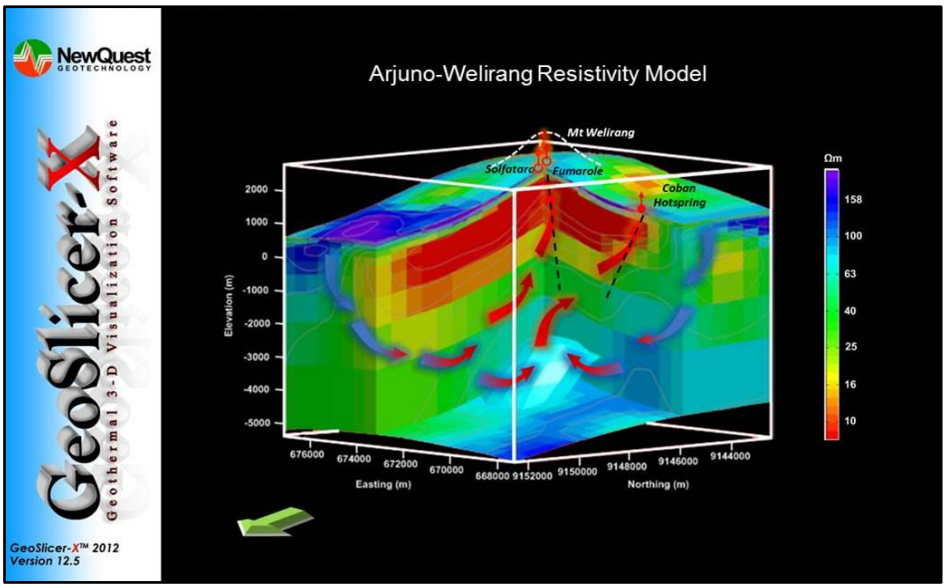

Figure 19: 3-D Resistivity Model Using GeoSlicer-X Software of the Arjuno-Welirang Geothermal Area (Daud et al., 2015).

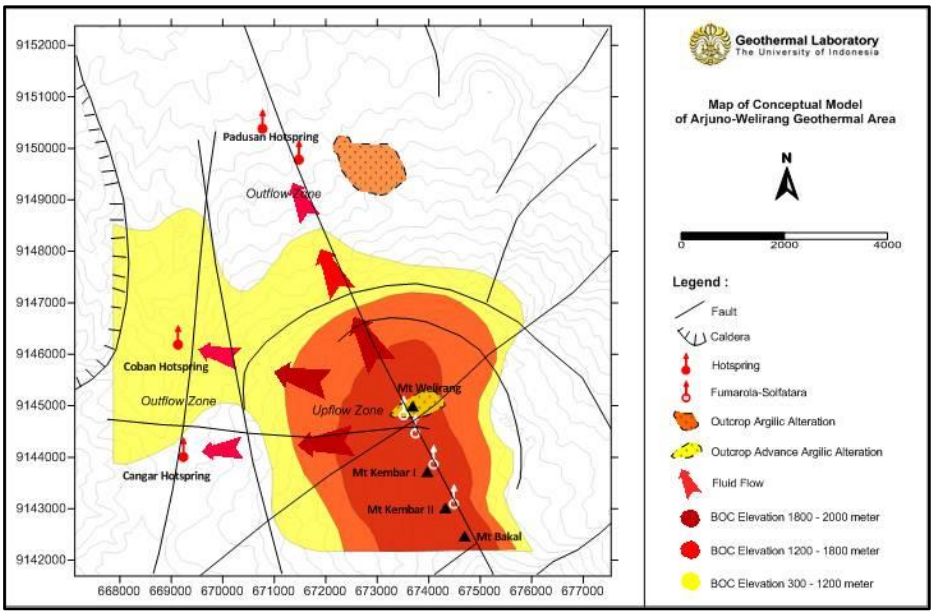

Figure 20: Conceptual Model Represented by BOC Elevation Contour and Hydrogeology Map of the Arjuno-Welirang Geothermal Area (Daud et al., 2015).

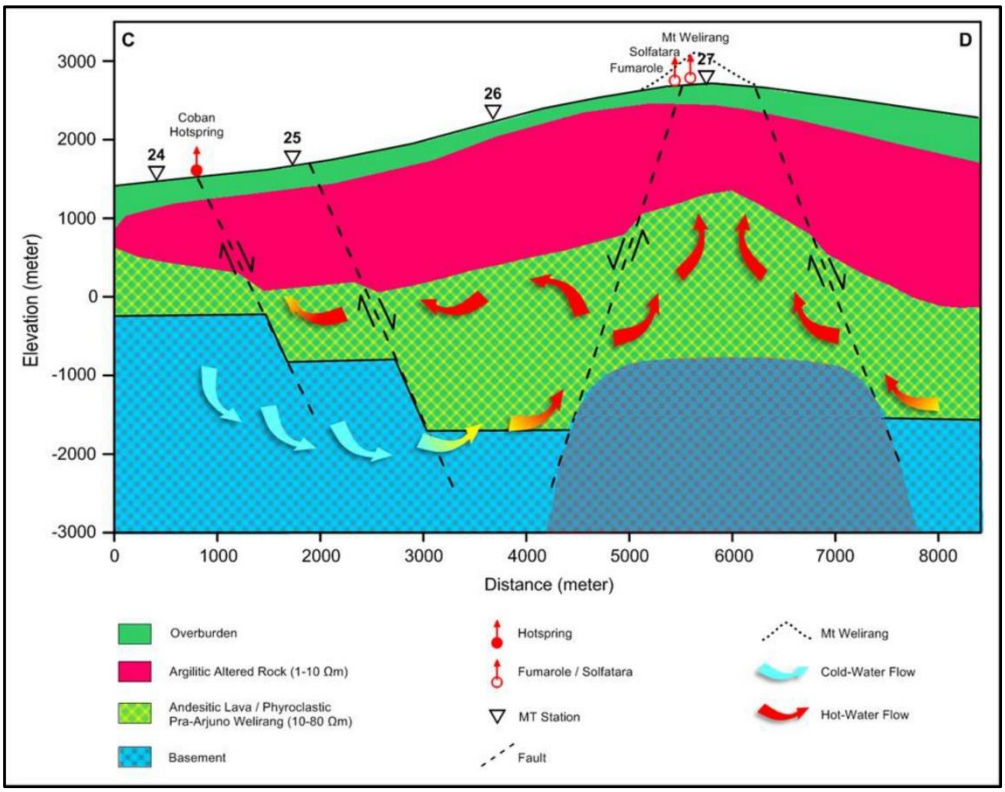

Figure 21: Conceptual Model of the Arjuno-Welirang Geothermal System (Daud et al., 2015).